Environmental Science & Technology

Article

pubs.acs.org/est

Impact of Iron Precipitant on Toxicity of Arsenic in Water: A Combined in Vivo and in Vitro Study

Su Liu, Xuechao Guo, Xuxiang Zhang, Yibin Cui, Yan Zhang, and Bing Wu*

State Key Lab of Pollutant Control and Resource Reuse, School of the Environment, Nanjing University, Nanjing, 210023, P.R. China

Supporting Information

ABSTRACT: Removing arsenic (As) from drinking water is widely dependent on iron (Fe)-based coagulation/flocculation techniques. However, little is known about the influence of Fe precipitant on As toxicity. In this present study, the influence of Fe on As toxicity was determined at systems biology level by in vitro and in vivo experiments. In vitro study based on HepG2 cell line found that Fe increased the As toxicity on cell viability and DNA damage, indicating the synergetic toxic effects. However, when the Fe and As were simultaneously exposed to mice by drinking water for 90 days, the results showed that Fe reduced the changes of hepatic transcriptomic profiles and serum and urine metabolic profiles caused by As exposure, showing the antagonistic toxic effects. The antagonistic effects might be because Fe reduced As bioavailability and accumulation, which was verified by As and Fe levels in feces and liver. The results of this study indicate that Fe precipitant can influence the As toxicity. The interactions between As and Fe and their bioavailability might play important roles in the As toxicity. When assessing the safety of As in drinking water, it is necessary to fully consider the combined effects of As and Fe.

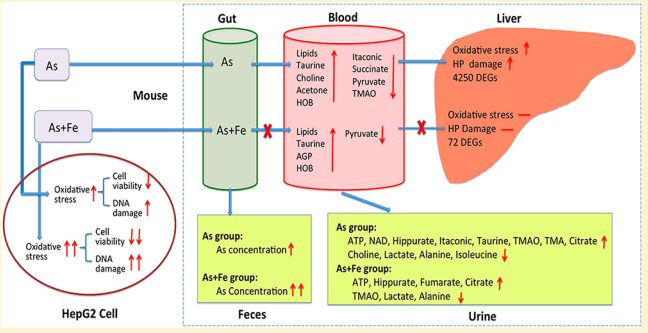

INTRODUCTION

Arsenic (As) represents a global environmental health threat. Epidemiological studies and clinical observations indicate that As is associated with an increased incidence of human cancer of the skin, liver, kidney, lung, prostate, and urinary bladder.[1−3] As can be exposed to humans via drinking water and foods.[4,5] Its safety in drinking water is a major concern in many countries around the world, such as Bangladesh, India, Mongolia, China, Poland, Hungary, Chile, and Argentina.[6,7] To effectively protect human health, the maximum contaminant level of As in drinking water was reduced from 50 to 10 μg/L in many countries.[8]

A variety of treatment processes have been developed for As removal from contaminated water. Of these processes, the most promising are coagulation/flocculation and adsorption because of their low cost and high efficiency.[9−11] Coagulation/flocculation, mainly using iron (Fe) or aluminum salts as coagulants, can convert soluble As species into insoluble reaction products. The treatment systems have been discussed in many studies. Some conclusions are available: Fe precipitants are more effective than aluminum, titanium, and zirconium ones. Solid surface of Fe has a strong affinity with negatively charged arsenite/arsenate, and can form a strong bond.[12] At present, Fe-based processes have been widely applied in the actual treatment of As-contaminated water.

The safety of using Fe precipitants to remove As from water has been mainly discussed based on the concentration and toxicity of As. Fe was rarely considered because of its low toxicity. However, it has been proven that Fe in blood and organs can influence As toxicity.[13,14] Reactive oxygen species (ROS) induction by As is one of the main mechanisms of As toxicity.[15−18] As can release redox-active Fe from ferritin. The free Fe plays a central role in generating harmful oxygen species by promoting the conversion of $O_2\bullet-$ and H_2O_2 into highly reactive •OH, which could induce oxidative stress and damage.[19−23] Therefore, it is important to determine the toxicity of Fe and As oral coexposure to evaluate the safety of As treatment process by Fe precipitants. Poddar et al. found that ferrous sulfate could reduce the clastogenic effects of As in mice.[24] Recently, Chandrasekaran et al. investigated the acute effects of combined As and Fe on rat livers by gavage, and found their synergetic effects on hepatic oxidative damage.[25] However, both researches just determined the acute effects of Fe and As coexposure at high levels, and paradoxical results were obtained. Little is known about the toxic effects and mechanism of actions of Fe and As coexposure at low levels by long-term exposure.

The aim of this research is to study the combined effects of Fe and As by in vitro and in vivo experiments. First, the cytotoxicity and genotoxicity of combined As and Fe on human hepatoma cell line HepG2 were determined. Then, we analyzed the As and Fe bioaccumulation, histopathological changes, oxidative stress, transcriptomic profiles, and metabonomic

Received: January 12, 2013
Revised: March 3, 2013
Accepted: March 8, 2013
Published: March 8, 2013

   dx.doi.org/10.1021/es400176m | Environ. Sci. Technol. 2013, 47, 3432−3438

profiles of mice exposed to As, Fe, and their combination by drinking water. The combined effects of As and Fe based on in vitro and in vivo experiments are systematically discussed to determine the influence of Fe precipitant on the As toxicity. This study provides new insight into the health risk assessment of As removal by Fe-based techniques.

MATERIALS AND METHODS

Cell Culture and Assessment of Cytotoxicity. Human hepatoma cell line HepG2 obtained from KeyGEN Biotech (China) was maintained in Dulbecco's Modified Eagles Medium (DMEM) with 10% fetal bovine serum under standard cell culture conditions (37 °C, and 5% CO_2). The cytotoxicities of As (20 and 40 μM), Fe (10, 100, and 500 μM) and combined As and Fe were determined by cell counting kit-8 (CCK-8, Dojindo Molecular Technologies, Inc. Japan). Arsenic oxide was obtained from NSI Solution Inc. Ferric chloride was obtained from Sigma Chemical Co. HepG2 at a density of 5000 cells per well was seeded in a 96-well ELISA microplate. The cells were incubated for 24 h. After 24 h, target chemicals were added into the well. The cells were incubated for 24 h. Then, 10 μL of CCK-8 solution was added into each well of the plate. After incubating the plate for 1 h, spectrophotometric measurement of the mixture was performed in a microplate reader (Bio-Tek) at a wavelength of 450 nm. Based on the absorbance, the cell viability was calculated.

Comet Assay. The levels of DNA strand break in HepG2 were determined by comet assay using the method described by our previous report.[26] Electrophoresis was conducted at 20 °C using 25 V and 300 mA for 25 min. After electrophoresis, the gels were washed three times with 0.5 M Tris buffer (pH 7.5). The slides were stained with ethidium bromide, and covered with coverslips. The stained slides were examined with a fluorescent microscope (BX41, Olympus, Japan). Three slides per group were prepared and at least 50 cells were analyzed for each slide. Photos were taken with a digital camera (C-5050ZOOM, Olympus, Japan). Images were analyzed by CASP software, and olive tail moment of each comet was calculated to indicate the level of DNA damage.

Animal Treatment. Five-week-old male mice (*Mus musculus*, ICR) were purchased from the experimental animal center of Academy of Military Medical Science of China and housed in stainless-steel cages. Ambient conditions were 25 ± 3 °C, 50 ± 5% relative humidity, and a 12/12 h light/dark cycle. Following acclimated for one week, forty mice (18.01 ± 0.91 g) were randomly assigned to control and three treated groups (ten mice in one group). For the control group, mice were fed with pure water. For three treated groups, based on the As and Fe levels in the real water and water treatment processes,[1,10,27−29] mice were fed with 3 mg/L As, 5 mg/L Fe, and 3 mg/L As + 5 mg/L Fe, respectively. All the mice had free access to food and water. The exposure period was 90 days. During exposure, As and Fe concentrations in exposure water were determined by atomic fluorescence spectrometry (AFS) and atomic absorption spectrometer (AAS), respectively. Urine and fecal pellets from each mouse were separately collected in 1.5-mL microfuge tubes and immediately frozen in −20 °C. Urine samples were obtained on days 30 and 90, and feces samples were obtained on day 90. After exposure, mice were anesthetized with diethyl ether. Blood was collected by eyeball removal and immediately put into ice-cold tubes. Serum was separated by centrifugation at 3000 rpm for 15 min. Urine and serum samples were kept in −80 °C until use. All experimental processes were in accordance with NIH Guide for the Care and Use of Laboratory animals.

Histopathological Analysis. Parts of liver and kidney were taken and fixed in 10% formalin solution. After 24−28 h the organ samples were dehydrated in a grade alcohol series and embedded in paraffin wax. Sections of 4−5 μm thickness were stained with hematoxylin-eosin (H&E) for pathological studies.

Oxidative Stress Analysis. Hepatic oxidative stress of mice was determined by measurement of superoxide dismutase (SOD), catalase (CAT), lipid peroxidation product malondialdehyde (MDA), and 8-OHdG.[30−32] For SOD, CAT, and MDA, part of left lobe of liver (300−500 mg) was homogenized, and supernatants were used for various estimations. The protein contents were determined using the modified method of Lowry et al.[33] The SOD, CAT activities, and MDA level were measured using commercial kits (Jiancheng, China). For 8-OHdG levels, genomic DNA of mouse livers (left lobe) was isolated by Genomic DNA Mini Preparation Kit (Beyotime, China), and the 8-OHdG levels were determined using a mouse 8-OHdG enzyme-linked immunosorbent assay (ELISA) kit (Jiancheng, China). Each experiment was performed in triplicate.

Transcriptomic Analysis of Mouse Liver. RNA from left hepatic lobe of each mouse in one group was separately extracted and cleaned using Trizol reagent protocol (Invitrogen, USA) and Qiagen RNeasy miniRNA cleanup protocol (Qiagen, USA), respectively. Nine mice per group were randomly divided into three sets (three mice per set), and an equal amount of RNAs from mice in the same set was pooled into one single sample for microarray analysis. A total of three GeneChip Mouse Gene 1.0 ST arrays (Affymetrix, USA) for every group was applied. Processes for microarray analysis, including synthesis of double-strand cDNA, labeled transcript and fragment, hybridization, washing, staining, and scanning of hybridization products, were carried out according to manufacture's protocol of Affymetrix.[34]

Normalization and comparison analysis of probe values were performed by Expression Console software (Affymetrix, USA). Differentially expressed genes (DEGs) in treated groups were identified by statistical p-value ($p < 0.05$) and fold change ($\geq \pm 2$). Biological meanings of DEGs were analyzed by pathway analysis. DEGs were mapped into different biological pathways according to the Kyoto encyclopedia of genes and genomes (KEGG) pathway database (http://www.genome.ad.jp/kegg/pathway.html) using SBC Analysis System of Shanghai Biotechnology Corporation (http://sas.ebioservice.com/). The significantly altered KEGG pathways were identified based on the criteria that have 3 or more DEGs, and a hypergeometric test with $p \leq 0.01$.

Metabonomic Analysis of Serum and Urine. Serum and urine samples were thawed and filtered twice using microcentrifuge filters to remove proteins. For serum preparation, 75 μL of pH 7.4 phosphate buffer and 75 μL of D_2O containing 0.1% of NaN_3 and 0.05% of TSP were added to 350 μL of serum. For urine preparation, 225 μL of phosphate buffer was added to 225 μL urine along with 50 μL of D_2O containing NaN_3 and TSP. The prepared serum and urine samples were transferred into Bruker 1.7-mm NMR tubes. The metabolites in serum and urine were analyzed by ^{1}H NMR spectroscopy using a Bruker 600 MHz spectrometer (Bruker, Germany).

Fourier transformed ^{1}H NMR spectra were manually phased and baseline was corrected using MestReC software (MestreC Research, Spain). Each spectrum was segmented into 0.005-

ppm bins. Water resonances (5.0−4.5 ppm) and urea resonances (6.0−5.5 ppm) were removed from data sets prior to normalization. Partial least-squares discriminant analysis (PLS-DA) was used to explore the main effects in NMR data sets by SIMCA-P software (Umetric, Sweden). Statistical differences of metabolites among groups were evaluated using one-way analysis of variance (ANOVA) test followed by Tukey's post hoc test. All analyses were performed by SPSS 15 software (SPSS Inc., USA). A probability value <0.05 was accepted as significance.

RESULTS AND DISCUSSION

Cytotoxicity and Genotoxicity of HepG2. Based on previous reports on As and Fe cytotoxicity,[35,36] we chose their concentrations used in this study. The results of cytotoxicity and genotoxicity in HepG2 are shown in Figure 1. There was no cytotoxicity for exposure of Fe alone. The cell viabilities of HepG2 exposed to 20 and 40 μM As were 68.5% and 58.6%, respectively, indicating the As induced the cytotoxicity of HepG2. When As and Fe were simultaneously exposed to HepG2, compared with the exposure of As alone, the cell viabilities were dramatically reduced, which suggested that Fe could increase the cytotoxicity of As. Moreover, the synergetic effects were also found in the DNA damage of HepG2. Comet assay found that Fe increased the levels of DNA strand break caused by As (Figure 1b and c). Thus, we deduce that Fe might increase the As toxicity, and there are synergetic toxic effects for As and Fe coexposure. However, the in vitro experiments do not consider the adsorption, metabolism, and transportation of chemicals in organism, and cannot effectively reflect the actual adverse effects of chemicals. Therefore, we applied the mouse as model animal to further analyze the combined effects of As and Fe.

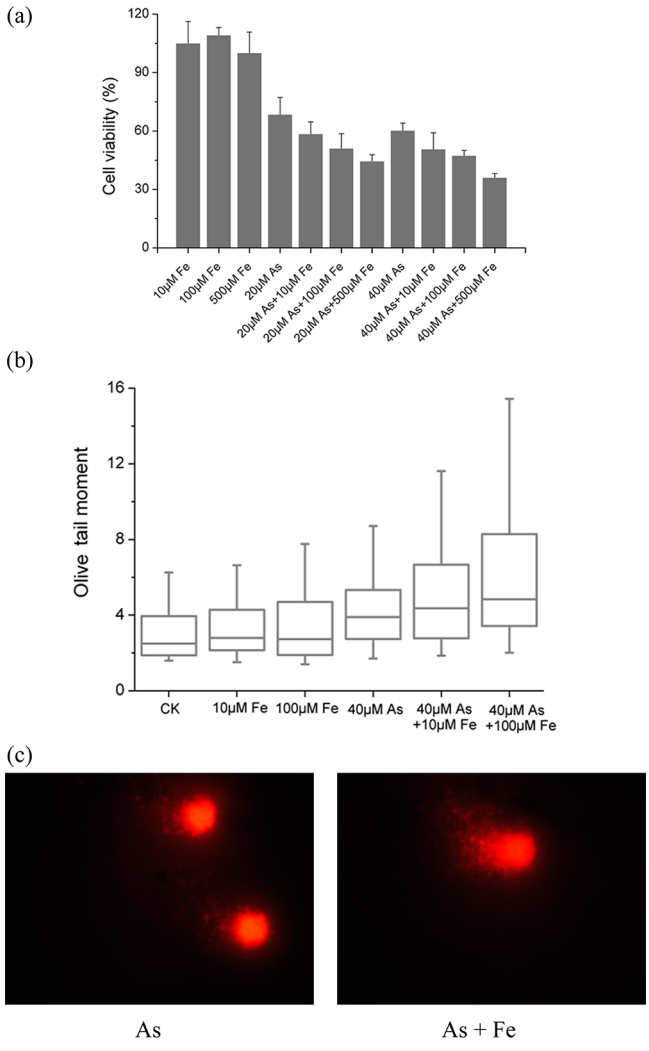

Figure 1. Cytotoxicity and genotoxicity of As and Fe exposure in HepG2 cell line: (a) cell viability of different exposures determined by cell counting kit-8; (b) olive tail moment (OTM) from comet assay, high OTM presents high DNA damage; (c) typical comet image of HepG2 exposed to As and As+Fe.

Water Intake and Organ Weight of Mice. During a 90-day exposure period, As and Fe concentrations in exposure water were measured; results are shown in Supporting Information Table S1. As and Fe were not detected in the control group. For the Fe group, because of formation of $Fe(OH)_3$, the actual Fe concentration (3.35−4.83 mg/L) in solution was lower than the nominal value. For As and As+Fe groups, no obvious precipitation was found, and the measured As and Fe levels were close to the nominal values. Average daily water consumption of mice in one group (mean ± SD) was 59.94 ± 14.92, 52.33 ± 11.06, 60.57 ± 14.20, and 60.21 ± 19.79 mL/day for control, As, Fe, and As+Fe groups, respectively. No significant changes for daily water consumption among four groups were found ($p > 0.05$).

After 90 days, As, Fe, and As+Fe exposures did not induce significant changes of body weight or relative organ weight ($p > 0.05$) (Table S2). Moreover, we determined the histopathological changes of liver and kidney (Figure S1). For liver, hepatocellular necrosis and inflammatory infiltration were observed in mice exposed to As. No damage was found in mouse livers in Fe and As+Fe groups. For kidney, interstitial nephritis was observed in mice exposed to As alone and Fe alone. In addition, the vacuolation was also found in the Fe group. No obvious damage was found in mouse kidneys for the coexposure of As and Fe. These results showed that there were antagonistic effects for As and Fe on histopothological changes.

Bioaccumulation of As and Fe in Mouse Liver. The liver is an important organ of As accumulation and metabolism. It has been proved that the liver is a target of arsenic carcinogenesis.[37] Thus, the bioaccumulation and toxicity of As in liver were specifically evaluated in this study. After the 90-day exposure, the levels of As and Fe in mouse livers of control and treated groups were determined, which are shown in Figure 2. The highest Fe concentration in mouse livers was found in the Fe group. However, compared with control group, no significant change was found ($p > 0.05$). As concentration in mouse livers of As group was 71.25 ± 3.89 ng/g liver, which was significantly higher than that of control group ($p < 0.05$). No significant increases of As concentration were found in the As+Fe group. The results indicated that the Fe effectively reduced the As bioaccumulation in mouse livers. To further validate the conclusion, we measured the As levels in the feces and found that As levels in feces of As+Fe group were highest (Figure.2c), indicating more excretion of As.

Evaluation of Hepatic Toxicity. Hepatic toxicities of As and/or Fe exposures were characterized by changes of oxidative stress and transcriptomic profiles. Significant increases in SOD activity, MDA level, and 8-OHdG level in the As group were observed (Figure S2). For Fe and As+Fe groups, no significant changes were found ($p > 0.05$), which indicated that Fe

dx.doi.org/10.1021/es400176m | Environ. Sci. Technol. 2013, 47, 3432−3438

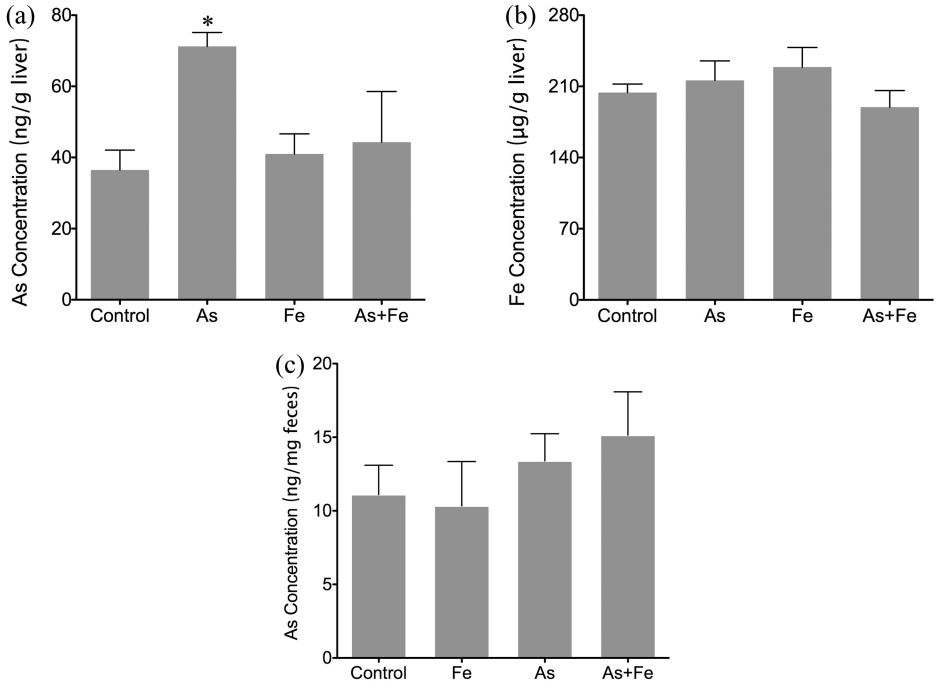

Figure 2. As and Fe concentrations in mouse livers and feces in control, As, Fe, and As+Fe groups. Values are mean values ± standard deviation. Statistical differences among groups were evaluated using ANOVA test followed by Tukey's post hoc test, $*p < 0.05$.

reduced the hepatic oxidative stress and damage caused by As exposure. For CAT activity, As, Fe, and As+Fe exposures could not induce its alteration.

Transcriptomic profiles of mouse livers were analyzed using Mouse Gene 1.0 ST Array. All data obtained from microarray analysis are publicly available at EBI's ArrayExpress Archive database (Accession E-MEXP-3763). A total of 4250, 498, and 72 genes were determined to be DEGs in As, Fe, and As+Fe groups, respectively. Most DEGs in treated groups were located in 2−3 fold (76.8−86.7%) and 3−4 fold (10.6−11.5%) (Figure S3). We compared the gene expressions of 72 DEGs in As+Fe group with those in As and Fe groups. The heat map is shown in Figure 3. Of 72 DEGs, expressions of 33 genes were similar to those in the As group, and expressions of 19 genes were similar to those in the Fe group. The results indicate that the gene expression profiles of mouse livers in As+Fe groups might be simultaneously influenced by Fe and As. However, the number of DEGs was significantly lower than that in As and Fe groups, indicating the antagonistic effects of Fe and As.

To characterize the biological meaning of DEGs, they were mapped into biological pathways. A total of 98, 10, and 4 biological pathways were significantly altered by exposure of As, Fe, and As+Fe, respectively. These different KEGG pathways were divided into two groups, i.e. biological process and metabolic pathway. The altered top 10 biological processes and metabolic pathways are shown in Tables S3 and 4S, respectively. For As exposure, some genes and pathways involved in inflammatory infiltration and oxidative stress were altered, including signal transduction, cell process, genetic information processing, and lipid metabolism. It has been proved that ROS generation associated with As exposure plays a fundamental role in the induction of adverse health effects and disease. ROS can activate/inactivate many signaling factors by oxidation of thiol groups and alter the intracellular redox state, consequently induce cell signaling pathways, downstream gene expression, and cell proliferation or death.[15,18] Combined

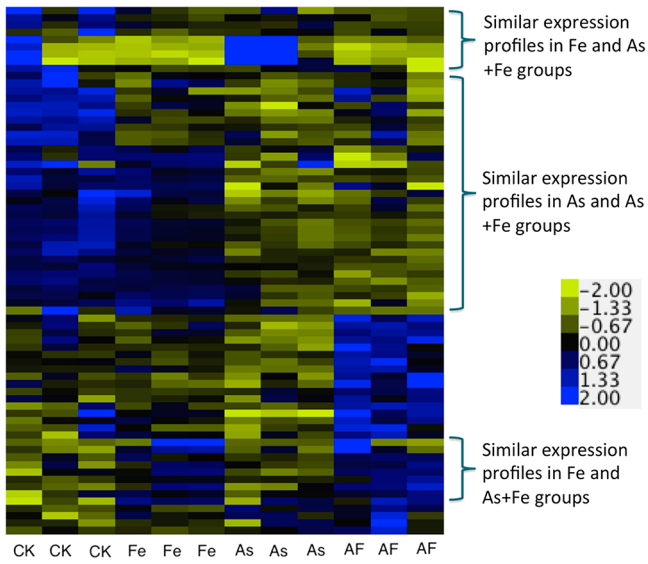

Figure 3. Heat map of 72 differentially expressed genes found in As +Fe group. Data were standardized, and hierarchical clustering was performed. Yellow represents low expression, and blue represents high expression. AF means the coexposure of As and Fe.

with the results of oxidative stress and histopathological analysis, the results of microarray analysis validate the conclusions that As can cause liver impairment, and oxidative stress and damage might be a potential mechanism for hepatotoxicity. For Fe exposure, although Fe exposure did not cause the histopathological changes and oxidative stress (Figure S1 and S2), some biological pathways involved in hepatic signal transduction, immune system, lipid metabolism, and energy metabolism were altered, suggesting that the adverse effects of Fe focused on the genotype of mouse livers. It is interesting that the coexposure of As and Fe did not induce significant alterations of transcriptomic profiles. Only signal

dx.doi.org/10.1021/es400176m | Environ. Sci. Technol. 2013, 47, 3432−3438

transduction and immune system were significantly changed (Table S3), and no altered metabolic pathways were found at transcriptomic level. Combined with the results of oxidative stress and histopathological analysis, we think that Fe and As in drinking water exert antagonistic toxic effects on mouse livers under the exposure conditions used in this study. The antagonistic effects might be attributed to the fact that the Fe reduced the As accumulation in the mouse livers of As+Fe group (Figure 2).

Evaluation of Metabolic Profiles. Metabolic profiles of serum and urine can reflect the influence of the transport and excretion of xenobiotics. Therefore, the serum and urine metabolites were determined in this study. To characterize the variations of metabolic profiles associated with treatment process, a PLS-DA model using one orthogonal component and three predictive components was carried out on all individuals. Good discriminations on serum and urine metabolites were observed among the four groups (Figure 4). For serum, a total of 9, 9, and 5 metabolites were significantly changed in As, Fe, and As+Fe groups, respectively (Table S5).

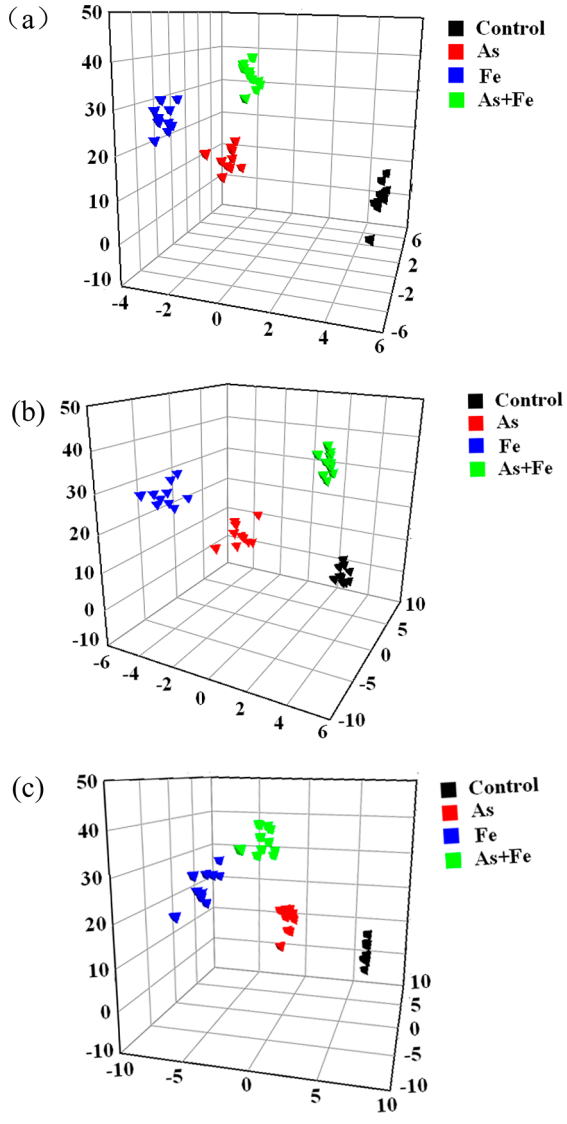

Figure 4. Partial least-squares discriminant analysis of serum and urine metabolites determined by ^{1}H NMR: (a) serum samples on day 90; (b) urine samples on day 30; (c) urine samples on day 90.

For urine, on day 30, a total of 5, 9, and 3 altered metabolites were found in As, Fe, and As+Fe groups, respectively. After 90-day exposure, the number of altered metabolites for As, Fe, and As+Fe groups increased to 12, 12, and 7, respectively (Table S6). The increases of altered metabolites indicated that the As or/and Fe exposure induced the changes of urine metabolites. Among three treated groups, the exposure of As or Fe alone induced more changes of metabolites in serum and urine than coexposure of As and Fe, suggesting the antagonistic effects on metabolic profiles. The results were consistent with the results of hepatic toxicity.

This study found that As, Fe, and As+Fe exposures all significantly altered the carbohydrate metabolism (such as pyruvate, NAD^{+}, succinate, and hippurate), lipid and fatty acid metabolism (such as choline, TMAO, TMA, and lipids), and amino acid metabolism (such as taurine, glutamine, alanine, and histidine). The changes of metabolites in As+Fe group indicated that the coexposure of As and Fe induced the adverse effects at metabolic levels. Of these metabolites, some host-gut microbiota cometabolites, such as hippurate, pyruvate, lacate, and TMA were found in the altered serum and urine metabolites. Alterations of host-gut microbiota cometabolites were previously reported as a consequence of the perturbation in gut microbiota.[38−41] For example, hippurate is a well-described mammalian microbial cometabolite, which can be derived from 3-phenylpropionic acid, a product of the gut microflora. TMA is a gut bacterial product of the choline. Therefore, we think that the perturbation of gut microbiota associated with coexposure of As and Fe could make a profound contribution to the altered metabolic profiles of mouse serum and urine, which need to be fully analyzed in the future research.

Compared Analysis of in Vitro and in Vivo Toxicity. When As and Fe was coexposed, the different combined effects were found in in vitro and in vivo experiments. The in vitro experiment based on HepG2 indicated that Fe could enhance the toxicity of As. However, in vivo experiment based on mice found that Fe reduced the toxicity of As. We systemically analyze these results, and construct the possible mechanism of the different toxicities (Figure 5).

It has been proved that As can release redox-active Fe from ferritin, which causes the ROS generation and oxidative damage.[17,21] When As and Fe is coexposed to HepG2, the increase of free Fe improves the generation of ROS, which might be the main reason of synergetic effects of As and Fe coexposure on cell viability and DNA damage. To further verify the explanation, we detected the antioxidant response of HepG2 by measuring SOD activity and glutathione (GSH) level. The results showed that coexposure of As and Fe enhanced the inducement of SOD and depletion of GSH (Figure S4). The results provide the indirect evidence that coexposure of As and Fe generates more reactive species, which can increase the cytotoxicity and genotoxicity.

When As and Fe are coexposed to mouse, As and Fe will be first adsorbed in gut. The increase of As level in feces and decrease in liver give the evidence that the Fe disturbs the adsorption of As. Although the interaction between Fe and As in gut and the roles of gut microbiota are not clear and need to be further studied, the reduction of As bioavailability should be the main reason of the low hepatic toxicity under coexposure of As and Fe. On the other hand, As and Fe in gut could directly act on the gut microbiota. Their changes in metabolism,

dx.doi.org/10.1021/es400176m | Environ. Sci. Technol. 2013, 47, 3432−3438

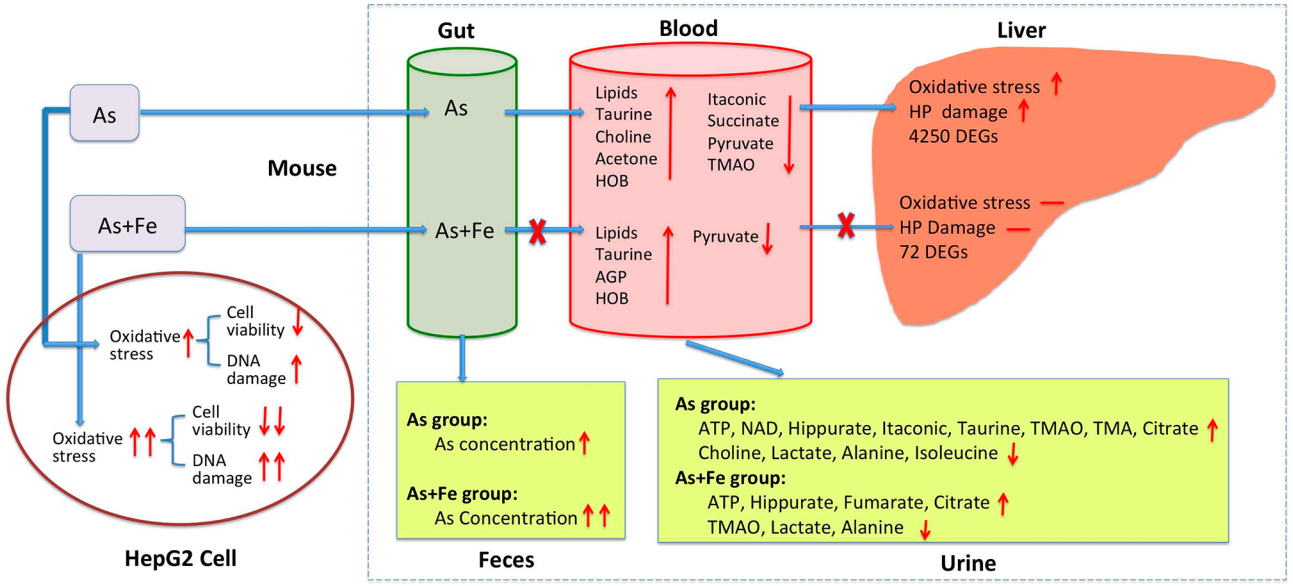

Figure 5. Comparison of toxic effects in HepG2 cell and mouse exposed to As alone and combined As and Fe. Red arrowhead indicates the increase or decease of toxic effects. The number of arrowheads presents the strength of toxic effects, i.e. two arrowheads indicate higher toxicity than one arrowhead. "−" Means that there are no toxic effects.

especially for the host-gut microbiota cometabolites, will influence the metabolic profiles of serum and urine.

In conclusion, upon coexposure of As and Fe on a cell line synergetic toxic effects exist. However, an animal experiment shows that Fe precipitant could reduce the As toxicity by changing the As adsorption and bioavailability. Our results support the viewpoint that, when assessing the safety of As in drinking water after Fe-based treatment process, their combined toxic effects need to be fully considered. Even if the As level in the drinking water is high, the existence of Fe might significantly change the As toxicity, just like the exposure conditions of this study. Although our study chose only one As and Fe level to research, and further research is needed to fully understand their combined effects, this study provides insight into the influence of Fe precipitant on As toxicity and a basis for future research aiming to understand combined toxicities on As and Fe in drinking water, which are very useful to practical engineering on As removal and mechanism of actions of As toxicity.

■ ASSOCIATED CONTENT

Supporting Information

Additional tables and figures. This material is available free of charge via the Internet at http://pubs.acs.org.

■ AUTHOR INFORMATION

Corresponding Author

*Tel. and fax: 86-25-89680720; e-mail: bwu@nju.edu.cn; mail: No.163 Xianlin Road, Nanjing, P.R. China.

Notes

The authors declare no competing financial interest.

■ ACKNOWLEDGMENTS

This research was supported by grants from the National Natural Science Foundation of China (51148003, 51208250), Foundation of State Key Laboratory of Pollution Control and Resource Reuse, and Science Foundation of Nanjing University.

■ REFERENCES

(1) Smith, A. H.; Steinmaus, C. M. Health effects of arsenic and chromium in drinking water: Recent human findings. *Annu. Rev. Public Health* **2009**, *30*, 107−122.

(2) Benbrahim-Tallaa, L.; Waalkes, M. P. Inorganic arsenic and human prostate cancer. *Environ. Health Perspect.* **2008**, *116* (2), 158−164.

(3) Yoshida, T.; Yamauchi, H.; Sun, G. F. Chronic health effects in people exposed to arsenic via the drinking water: Dose-response relationships in review. *Toxicol. Appl. Pharmacol.* **2004**, *198* (3), 243−252.

(4) Lubin, J. H.; Beane Freeman, L. E.; Cantor, K. P. Inorganic arsenic in drinking water: An evolving public health concern. *J. Natl. Cancer Inst.* **2007**, *99* (12), 906−907.

(5) Mandal, B. K.; Suzuki, K. T. Arsenic round the world: A review. *Talanta* **2002**, *58* (1), 201−235.

(6) Schuhmacher-Wolz, U.; Dieter, H. H.; Klein, D.; Schneider, K. Oral exposure to inorganic arsenic: Evaluation of its carcinogenic and non-carcinogenic effects. *Crit. Rev. Toxicol.* **2009**, *39* (4), 271−298.

(7) Bundschuh, J.; Litter, M. I.; Parvez, F.; Roman-Ross, G.; Nicolli, H. B.; Jean, J. S.; Liu, C. W.; Lopez, D.; Armienta, M. A.; Guilherme, L. R.; Cuevas, A. G.; Cornejo, L.; Cumbal, L.; Toujaguez, R. One century of arsenic exposure in Latin America: A review of history and occurrence from 14 countries. *Sci. Total Environ.* **2012**, *429*, 2−35.

(8) Smith, A. H.; Lopipero, P. A.; Bates, M. N.; Steinmaus, C. M. Public health - Arsenic epidemiology and drinking water standards. *Science* **2002**, *296* (5576), 2145−2146.

(9) Giles, D. E.; Mohapatra, M.; Issa, T. B.; Anand, S.; Singh, P. Iron and aluminium based adsorption strategies for removing arsenic from water. *J. Environ. Manage.* **2011**, *92* (12), 3011−3022.

(10) Mohan, D.; Pittman, C. U., Jr. Arsenic removal from water/wastewater using adsorbents–A critical review. *J. Hazard. Mater.* **2007**, *142* (1−2), 1−53.

(11) Song, S.; Lopez-Valdivieso, A.; Hernandez-Campos, D. J.; Peng, C.; Monroy-Fernandez, M. G.; Razo-Soto, I. Arsenic removal from high-arsenic water by enhanced coagulation with ferric ions and coarse calcite. *Water Res.* **2006**, *40* (2), 364−372.

(12) Pallier, V.; Feuillade-Cathalifaud, G.; Serpaud, B.; Bollinger, J. C. Effect of organic matter on arsenic removal during coagulation/flocculation treatment. *J. Colloid Interface Sci.* **2010**, *342* (1), 26−32.

(13) Paul, P. C.; Misbahuddin, M.; Ahmed, A. N.; Dewan, Z. F.; Mannan, M. A. Accumulation of arsenic in tissues of iron-deficient rats. *Toxicol. Lett.* **2002**, *135* (3), 193−197.
(14) Rahman, M. M.; Rahman, F.; Sansom, L.; Naidu, R.; Schmidt, O. Arsenic interactions with lipid particles containing iron. *Environ. Geochem. Health* **2009**, *31* (Suppl 1), 201−206.
(15) De Vizcaya-Ruiz, A.; Barbier, O.; Ruiz-Ramos, R.; Cebrian, M. E. Biomarkers of oxidative stress and damage in human populations exposed to arsenic. *Mutat. Res., Genet. Toxicol. Environ. Mutagen.* **2009**, *674* (1−2), 85−92.
(16) Kitchin, K. T.; Conolly, R. Arsenic-Induced Carcinogenesis-Oxidative Stress as a Possible Mode of Action and Future Research Needs for More Biologically Based Risk Assessment. *Chem. Res. Toxicol.* **2010**, *23* (2), 327−335.
(17) Chowdhury, R.; Chatterjee, R.; Giri, A. K.; Mandal, C.; Chaudhuri, K. Arsenic-induced cell proliferation is associated with enhanced ROS generation, Erk signaling and CyclinA expression. *Toxicol. Lett.* **2010**, *198* (2), 263−271.
(18) Ghatak, S.; Biswas, A.; Dhali, G. K.; Chowdhury, A.; Boyer, J. L.; Santra, A. Oxidative stress and hepatic stellate cell activation are key events in arsenic induced liver fibrosis in mice. *Toxicol. Appl. Pharmacol.* **2011**, *251* (1), 59−69.
(19) Kitchin, K. T.; Wallace, K. Evidence against the nuclear in situ binding of arsenicals-Oxidative stress theory of arsenic carcinogenesis. *Toxicol. Appl. Pharmacol.* **2008**, *232* (2), 252−257.
(20) Wang, W.; Knovich, M. A.; Coffman, L. G.; Torti, F. M.; Torti, S. V. Serum ferritin: Past, present and future. *Biochim. Biophys. Acta, Gen. Subj.* **2010**, *1800* (8), 760−769.
(21) Ahmad, S.; Kitchin, K. T.; Cullen, W. R. Arsenic species that cause release of iron from ferritin and generation of activated oxygen. *Arch. Biochem. Biophys.* **2000**, *382* (2), 195−202.
(22) Kitchin, K. T.; Wallace, K. The role of protein binding of trivalent arsenicals in arsenic carcinogenesis and toxicity. *J. Inorg. Biochem.* **2008**, *102* (3), 532−539.
(23) Meng, D.; Wang, X.; Chang, Q. S.; Hitron, A.; Zhang, Z.; Xu, M.; Chen, G.; Luo, J.; Jiang, B. H.; Fang, J.; Shi, X. L. Arsenic promotes angiogenesis in vitro via a heme oxygenase-1-dependent mechanism. *Toxicol. Appl. Pharmacol.* **2010**, *244* (3), 291−299.
(24) Poddar, S.; Mukherjee, P.; Talukder, G.; Sharma, A. Dietary protection by iron against clastogenic effects of short-term exposure to arsenic in mice in vivo. *Food Chem. Toxicol.* **2000**, *38* (8), 735−737.
(25) Chandrasekaran, V. R. M.; Muthaiyan, I.; Huang, P. C.; Liu, M. Y. Using iron precipitants to remove arsenic from water: Is it safe? *Water Res.* **2010**, *44* (19), 5823−5827.
(26) Wu, B.; Liu, S.; Guo, X.; Zhang, Y.; Zhang, X.; Li, M.; Cheng, S. Responses of Mouse Liver to Dechlorane Plus Exposure by Integrative Transcriptomic and Metabonomic Studies. *Environ. Sci. Technol.* **2012**, *46* (19), 10758−10764.
(27) Ahmed, M. K.; Habibullah-Al-Mamun, M.; Hossain, M. A.; Arif, M.; Parvin, E.; Akter, M. S.; Khan, M. S.; Islam, M. M. Assessing the genotoxic potentials of arsenic in tilapia (*Oreochromis mossambicus*) using alkaline comet assay and micronucleus test. *Chemosphere* **2011**, *84* (1), 143−149.
(28) Paul, D. S.; Walton, F. S.; Saunders, R. J.; Styblo, M. Characterization of the impaired glucose homeostasis produced in C57BL/6 mice by chronic exposure to arsenic and high-fat diet. *Environ. Health Perspect.* **2011**, *119* (8), 1104−1109.
(29) Baskan, M. B.; Pala, A. Determination of arsenic removal efficiency by ferric ions using response surface methodology. *J. Hazard. Mater.* **2009**, *166* (2−3), 796−801.
(30) Oberley, L. W.; Spitz, D. R. Assay of superoxide dismutase activity in tumor tissue. *Methods Enzymol.* **1984**, *105*, 457−464.
(31) Flohe, L.; Gunzler, W. A. Assays of glutathione peroxidase. *Methods Enzymol.* **1984**, *105*, 114−121.
(32) Yagi, K. Simple assay for the level of total lipid peroxides in serum or plasma. *Methods Mol. Biol.* **1998**, *108*, 101−106.
(33) Lowry, O. H.; Rosebrough, N. J.; Farr, A. L.; Randall, R. J. Protein measurement with the Folin phenol reagent. *J. Biol. Chem.* **1951**, *193* (1), 265−275.
(34) Wu, B.; Zhang, Y.; Zhao, D.; Zhang, X.; Kong, Z.; Cheng, S. Gene expression profiles in liver of mouse after chronic exposure to drinking water. *J. Appl. Toxicol.* **2009**, *29* (7), 569−577.
(35) Abiko, Y.; Shinkai, Y.; Sumi, D.; Kumagai, Y. Reduction of arsenic-induced cytotoxicity through Nrf2/HO-1 signaling in HepG2 cells. *J. Toxicol. Sci.* **2010**, *35* (3), 419−423.
(36) Alp, O.; Zhang, Y. F.; Merino, E. J.; Caruso, J. A. Selenium effects on arsenic cytotoxicity and protein phosphorylation in human kidney cells using chip-based nanoLC-MS/MS. *Metallomics* **2011**, *3* (5), 482−490.
(37) Liu, J.; Waalkes, M. P. liver is a target of arsenic carcinogenesis. *Toxicol. Sci.* **2008**, *105* (1), 24−32.
(38) Yap, I. K.; Li, J. V.; Saric, J.; Martin, F. P.; Davies, H.; Wang, Y.; Wilson, I. D.; Nicholson, J. K.; Utzinger, J.; Marchesi, J. R.; Holmes, E. Metabonomic and microbiological analysis of the dynamic effect of vancomycin-induced gut microbiota modification in the mouse. *J. Proteome Res.* **2008**, *7* (9), 3718−3728.
(39) Claus, S. P.; Ellero, S. L.; Berger, B.; Krause, L.; Bruttin, A.; Molina, J.; Paris, A.; Want, E. J.; de Waziers, I.; Cloarec, O.; Richards, S. E.; Wang, Y.; Dumas, M. E.; Ross, A.; Rezzi, S.; Kochhar, S.; Van Bladeren, P.; Lindon, J. C.; Holmes, E.; Nicholson, J. K. Colonization-induced host-gut microbial metabolic interaction. *mBio* **2011**, *2* (2), e00271−10.
(40) Martin, F. P.; Sprenger, N.; Montoliu, I.; Rezzi, S.; Kochhar, S.; Nicholson, J. K. Dietary modulation of gut functional ecology studied by fecal metabonomics. *J. Proteome Res.* **2010**, *9* (10), 5284−5295.
(41) Nicholson, J. K.; Holmes, E.; Kinross, J.; Burcelin, R.; Gibson, G.; Jia, W.; Pettersson, S. Host-gut microbiota metabolic interactions. *Science* **2012**, *336* (6086), 1262−1267.